

Tidal heating in a subsurface magma ocean on Io revisited

B. Aygün¹ and O. Čadek¹

¹Department of Geophysics, Faculty of Mathematics and Physics, Charles University,
Prague, Czech Republic

Key Points:

- Comparison of the predicted dissipation patterns with the geological map indicates that Io underwent a large thermal runaway in the past.
- Due to the Coriolis effect, the degree-2 Love numbers for models with a magma ocean can depend on the harmonic order.
- The tidal Love numbers are not sensitive to the presence of a fluid magma ocean if the thickness of the fluid layer is less than 2 km.

Abstract

We investigate the tidal dissipation in Io's hypothetical fluid magma ocean using a new approach based on the solution of the 3D Navier-Stokes equations. Our results indicate that Io may have experienced a period of intense tidal heating ($\approx 10^4$ TW) accompanied by excessive volcanism in the equatorial region, leading to catastrophic resurfacing of the pre-existing terrain. Tidal heating in Io's magma ocean does not correlate with the distribution of hot spots, and is maximum for an ocean thickness of about 1 km and a viscosity of less than 10^4 Pa.s. Due to the Coriolis effect, the k_2 Love number can depend on the harmonic order. We show that the analysis of k_2 may not reveal the presence of a fluid magma ocean if the ocean thickness is less than 2 km. If the fluid layer is thicker than 2 km, $k_{20} \approx k_{22}/2 \approx 0.7$.

Plain Language Summary

Jupiter's moon Io is the most active volcanic body in the Solar System. Although it is generally accepted that Io's volcanic activity is driven by the heat generated by tidal friction, the origin and the distribution of tidal heating within Io's interior remain a subject of debate. Here we investigate the tidal dissipation in Io's hypothetical fluid magma ocean using a new approach based on the solution of the 3D Navier-Stokes equations. Our results indicate that Io may have experienced a period of intense tidal heating accompanied by excessive volcanism in the equatorial region, leading to catastrophic resurfacing of the pre-existing terrain. Tidal heating in Io's magma ocean does not correlate with the distribution of hot spots, and is maximum for an ocean thickness of about 1 km and a viscosity of less than 10^4 Pa.s. We also discuss the sensitivity of Io's gravity signature to the presence of a magma ocean and provide estimates of the tidal Love numbers.

1 Introduction

Jupiter's moon Io is the most active volcanic body in the Solar System, with more than 400 known volcanoes, 150 of which are erupting at any given time (e.g., Schenk et al., 2001; Radebaugh et al., 2001; Veeder et al., 2012). Io's volcanic activity is driven by the heat generated by tidal friction caused by its orbital resonance with Europa and Ganymede (Peale et al., 1979). The average endogenous heat production is estimated to be of the

43 order of 100 TW (e.g., Veeder et al., 1994; Spencer et al., 2000; Lainey et al., 2009), which
44 is significantly more than the heat output of the Earth.

45 The dissipative response of the body to tidal forcing is determined by its internal
46 structure, size and the frequency of forcing. Dissipation of tidal energy can occur in dif-
47 ferent ways, in both the solid and liquid regions of the body. In a solid material, the dis-
48 sipative properties depend on the composition, temperature and structural character-
49 istics (grain size, melt content, etc.), while the dissipation in a liquid is controlled by a
50 single parameter, viscosity, varying with temperature and composition.

51 Physical models of solid body tides on Io usually assume that most of the heat is
52 generated in a partially molten layer beneath Io's lithosphere or in a deeper, potentially
53 dissipative mantle (e.g., Ross & Schubert, 1985; Segatz et al., 1988; Bierson & Nimmo,
54 2016; Hamilton et al., 2013; Renaud & Henning, 2018; Steinke et al., 2020; Kervazo et
55 al., 2021). The presence of a partially molten layer in Io's upper mantle is predicted by
56 the models of magmatic heat transfer (e.g., Moore, 2001, 2003; Steinke et al., 2020; Spencer
57 et al., 2020) and is consistent with the estimates of eruption temperatures indicating that
58 a substantial portion of Io's mantle is partially molten, with porosity between 3%-25%
59 (Keszthelyi et al., 2007).

60 An alternative model to explain Io's heat output has been proposed by Tyler et
61 al. (2015). The model assumes that the tidal heating is concentrated in a hypothetical
62 magma ocean that is approximated by a fluid layer. The main difference between the
63 solid and fluid tides is that the tidal deformation of a fluid layer is affected by the Cori-
64 olis force, an effect that is negligible in solid tide models. Tyler et al. (2015) shows that
65 fluid-tide models predict different patterns of tidal heating than solid-tide models and
66 can explain Io's heat production over a wide range of plausible parameters.

67 The existence of a magma ocean on Io was predicted by Peale et al. (1979), shortly
68 before the Voyager 1 mission discovered Io's active volcanism (Smith et al., 1979). At
69 the same time, the mission revealed mountains with elevations of ~ 10 km, suggesting
70 that Io must have a cold lithosphere (O'Reilly & Davies, 1981) that is significantly thicker
71 than that proposed by Peale et al. (1979). Although the concept of a mushy magma ocean
72 was supported by geological analysis (Keszthelyi et al., 1999), some scientists remained
73 skeptical and argued that heat transport by melt segregation would lead to rapid cool-
74 ing, reducing the melt fraction and preventing the formation of a magma ocean (e.g., Moore,

2001). The question of whether Io has a magma ocean was reopened in 2011 when Khurana and co-workers analyzed the magnetometer data collected by the Galileo spacecraft near Io and showed that the data were consistent with the presence of a global conductive layer. Taking into account the electrical properties of partially molten rocks, Khurana et al. (2011) interpreted this layer as a magma ocean with a thickness exceeding 50 km and a rock melt fraction of a few tens of percent. However, this model was challenged by Roth et al. (2017) and Blöcker et al. (2018) who argued that the interaction of the Jovian magnetosphere with Io’s plasma environment is a more likely explanation than a magma ocean. Recently, Miyazaki and Stevenson (2022) have explored the steady state of a solid layer with a high melt fraction (“magmatic sponge” with porosity >0.2). They showed that for a wide range of parameters such a layer would be unstable and it would swiftly separate into two phases, leading to the formation of a subsurface magma ocean. Such an ocean would likely contain some amount of crystals but it would behave rheologically as a liquid. The existence of a magma ocean does not contradict the results of Roth et al. (2017) and Blöcker et al. (2018) because the magma layer may be relatively thin ($\sim 1\text{--}10$ km) and the magnetic induction signal from Io’s interior may be weak compared to the magnetic field perturbations caused by the plasma interaction with Io’s asymmetric atmosphere.

In this study, we investigate the tidal dissipation in Io’s hypothetical magma ocean using a new approach based on the solution of the three-dimensional Navier-Stokes equations. Unlike the study of Tyler et al. (2015), where the mechanical coupling between the ocean and the solid parts of the moon was neglected, the flow in the ocean is calculated simultaneously with the deformation of the lithosphere and the sub-oceanic mantle. The resulting maps of tidal dissipation are compared with the geological evidence and the possible role of a magma ocean in Io’s thermal evolution is discussed.

2 Method

The models presented in this paper were obtained by solving the following set of equations:

$$\nabla \cdot \boldsymbol{\sigma} - 2\rho\boldsymbol{\omega} \times \mathbf{v} - \rho\nabla(V_t + V_g) = \rho \frac{d\mathbf{v}}{dt}, \quad (1)$$

$$\nabla \cdot \mathbf{v} = 0, \quad (2)$$

$$\frac{1}{\eta} \boldsymbol{\sigma}^d - \nabla \mathbf{v} - (\nabla \mathbf{v})^T + \frac{1}{\mu} \frac{\partial \boldsymbol{\sigma}^d}{\partial t} = \mathbf{0}, \quad (3)$$

108 where $\boldsymbol{\sigma}$ is the incremental stress tensor, ρ is the density, $\boldsymbol{\omega}$ is the angular frequency, V_t
 109 is the tidal potential, V_g is the gravitational potential due to the deformation, t is the
 110 time, \boldsymbol{v} is the velocity, $\boldsymbol{\sigma}^d$ is the deviatoric part of $\boldsymbol{\sigma}$, η is the dynamic viscosity, μ is the
 111 shear modulus and \bullet^T denotes the transpose of a tensor. Equation 1 is the momentum
 112 equation including the Coriolis force ($-2\rho\boldsymbol{\omega} \times \boldsymbol{v}$) and the time-varying tidal potential
 113 (Kaula, 1964),

$$114 \quad V_t(r, \theta, \phi, t) = V_{t,20}(r, t)P_{20}(\cos \theta) + V_{t,22}^c(r, t)P_{22}(\cos \theta) \cos 2\phi + V_{t,22}^s(r, t)P_{22}(\cos \theta) \sin 2\phi. \quad (4)$$

115 Here, r , θ and ϕ are the spherical coordinates, P_{20} and P_{22} are the associated Legendre
 116 functions, and

$$117 \quad V_{t,20} = \frac{3}{2}r^2\omega^2e \cos \omega t, \quad V_{t,22}^c = -\frac{3}{4}r^2\omega^2e \cos \omega t, \quad V_{t,22}^s = -r^2\omega^2e \sin \omega t, \quad (5)$$

118 where e is the eccentricity and ω is the angular speed. Equation 2 is the continuity equa-
 119 tion for an incompressible flow. Finally, equation 3 is the Maxwell constitutive law for
 120 a viscoelastic body expressed in terms of velocity \boldsymbol{v} . In the case of $\mu \rightarrow \infty$, the equa-
 121 tion reduces to a constitutive relation for a Newtonian fluid. We assume that the sur-
 122 face of the moon is free to move, the velocity and traction vectors are continuous at the
 123 internal interfaces and the core is in hydrostatic equilibrium.

124 Equations 1–3 are solved in the time domain using the semi-spectral method de-
 125 veloped by Aygün and Čadek (2023b). The spherical harmonic expansions are truncated
 126 at degree 20–200 depending on the viscosity of the magma ocean, while the spherical har-
 127 monic coefficients are discretized in 800 unevenly spaced radial points. The radial res-
 128 olution ranges from 1 m to 50 m in the magma ocean and from 100 m to 4 km in the
 129 rest of the mantle. Tidal dissipation (heat power per unit volume) is calculated using
 130 the formula (Souček et al., 2016)

$$131 \quad h(r, \theta, \phi) = \frac{1}{P} \int_{t_0}^{t_0+P} \frac{\boldsymbol{\sigma}^d : \boldsymbol{\sigma}^d}{2\eta} dt, \quad (6)$$

132 where P is the rotation period, t_0 is an arbitrary time and the symbol $:$ denotes the Frobe-
 133 nius inner product ($\sigma_{ij}^d \sigma_{ij}^d$ in the Cartesian components). The total dissipation or the
 134 total heat production, H , is calculated as the integral of h over the volume of the magma
 135 ocean. The spatial distribution of dissipation in Io’s magma ocean is presented in the
 136 form of maps showing the heating h integrated over the thickness of the ocean (“tidal
 137 heat flux”),

$$138 \quad q(\theta, \phi) = \frac{1}{R_m^2} \int_{R_m-d}^{R_m} h(r, \theta, \phi) r^2 dr. \quad (7)$$

139 where R_m and d are the outer radius and the thickness of the magma ocean, respectively.

140 The modeling approach used here is different from that used by Tyler et al. (2015)
141 in two main respects. First, the tidal response of the magma ocean is calculated by solv-
142 ing the three-dimensional (3D) Navier-Stokes equations, while Tyler et al. (2015) used
143 the Laplace tidal equations (LTE) where the tidal flow is described as a barotropic two-
144 dimensional sheet flow. Second, the response of Io to tidal loading is calculated not only
145 in the magma ocean but also in the lithosphere and the sub-oceanic mantle, which al-
146 lows us to precisely quantify the mechanical and gravitational coupling between the three
147 layers.

148 Our method is also more general than the methods used in studies investigating
149 the tidal response of water ocean worlds (e.g., Beuthe, 2016; Matsuyama et al., 2018; Rovira-
150 Navarro et al., 2019; Requier et al., 2019). To couple the flow in the ocean with the de-
151 formation of the crust, Beuthe (2016) and Matsuyama et al. (2018) proposed to solve
152 the LTE together with the equations governing the viscoelastic deformation of the over-
153 lying shell. Although their method is similar at first glance to our approach, it differs
154 from it in that the boundaries of the ocean are treated as free-slip surfaces and the flow
155 velocity does not change with radius. As recently shown by Aygün and Čadek (2023b),
156 the method by Beuthe (2016) correctly predicts the radially averaged flow in a thin ocean
157 layer but can lead to biased estimates of tidal heating. Unlike Beuthe (2016), Rovira-
158 Navarro et al. (2019) and Requier et al. (2019) determine the dissipation rate in the ocean
159 by using the 3D Navier-Stokes equations, but assume that the deformation of the crust
160 is not affected by the flow in the ocean and can therefore be imposed as a boundary con-
161 dition at the surface of the ocean. However, this assumption is valid only if the thick-
162 ness of the ocean layer is greater than about $0.01R_m \approx 15$ km, i.e., outside the thick-
163 ness range considered in the present study (Aygün & Čadek, 2023b).

164 The density structure of Io is chosen to match the total mass ($8.9319 \cdot 10^{22}$ kg) and
165 MoI factor (0.37685, Anderson et al., 2001) and to satisfy constraints on its material com-
166 position (Anderson et al., 1996). The upper boundary of the magma ocean is set to a
167 depth of 30 km and the thickness of the ocean is varied from 100 m to 10 km. We as-
168 sume that the magma behaves as a Newtonian liquid and its viscosity is constant through-
169 out the ocean. The viscosity of the magma ranges from 100 Pa s (hot mafic magma) to
170 10^7 Pa s (low-temperature magma with solid crystals suspended in the liquid phase, see,

171 e.g., Philpotts and Ague (2009)). For simplicity, we assume that the density of the magma
 172 is the same as the density of the mantle (for details, see table S1 in the Supporting In-
 173 formation (SI)).

174 The lithosphere and the mantle below the ocean are assumed to behave as a Maxwell
 175 viscoelastic solid. Since the main focus of this study is to examine tidal heating in a hy-
 176 pothetical magma ocean, the material parameters of the lithosphere and the sub-ocean
 177 mantle are chosen so that the tidal heat production outside the magma ocean is much
 178 smaller than Io’s current heat output.

179 **3 Results**

180 As illustrated in figure 1, the tidal flow in the magma ocean produces a wide va-
 181 riety of heating patterns and even small changes in ocean thickness can lead to order of
 182 magnitude changes in the total heat production. The heat flux distributions are sym-
 183 metric about the equator and most of them, but not all, also about the tidal axis. The
 184 heat flux patterns are dominated by dissipation at low latitudes, typical of fluid mod-
 185 els. The highest heat production ($> 10^4$ TW) is found in the case where tidal heating
 186 is concentrated in an equatorial zone at latitudes below 30° . This equatorial zone is clearly
 187 separated from the low-dissipation regions at higher latitudes and its position shows a
 188 remarkable correspondence with Io’s yellow bright plains (Williams et al., 2011). The
 189 strong zonal character of dissipation is unusual in the context of eccentricity tides and,
 190 to our knowledge, has not been reported in previous studies of tidal flow in subsurface
 191 (water or magma) oceans (e.g. Chen et al., 2014; Tyler et al., 2015; Matsuyama et al.,
 192 2018, 2022; Hay & Matsuyama, 2019). Although the purely zonal distribution of dissi-
 193 pation is obtained for models with a thin ocean ($d \approx 1$ km), the velocity field has a strong
 194 radial component ($v_r/v_\theta \approx v_r/v_\phi \approx 0.2$) that cannot be found by solving the LTE.
 195 The dependence of tidal heating on the thickness of the ocean and the viscosity of magma
 196 is shown in figure 2a. Inspection of the figure shows that the heat power of ~ 100 TW
 197 (Io’s observed heat output) is exceeded over a wide range of magma viscosities and ocean
 198 thicknesses, with maximum values achieved for $d \approx 1$ km and η between 10^2 and 10^4
 199 Pa.s. When d is significantly larger than 1 km, the 100 TW limit can only be achieved
 200 for $\eta > 10^4$ Pa.s. The results in figure 2a are qualitatively similar to those obtained from
 201 the solution of the Laplace tidal equations (figure 4a in Tyler et al. (2015)) but they dif-
 202 fer in three minor respects: First, the ocean thickness for which the maximum dissipa-

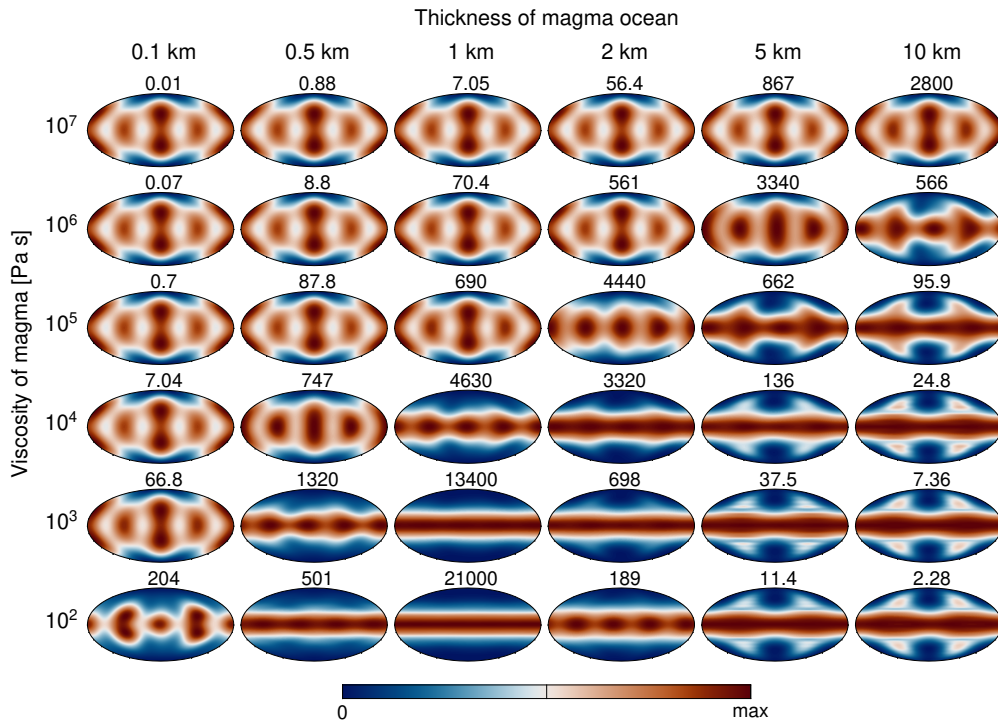


Figure 1. Distribution of tidal dissipation in the magma ocean, equation 7, evaluated for different thicknesses and viscosities of the ocean (Mollweide equal-area projection centered on 180° W longitude). The numbers above each map represent the total heat production of the magma ocean in TW.

203 tion is reached is about twice the value predicted by Tyler et al. (2015), second, no dis-
 204 sipation maxima are found for $d < 1$ km and third, the dissipation in the ocean van-
 205 ishes when $d \rightarrow 0$.

206 The tidal heating models discussed above were obtained under the assumption that
 207 Io’s solid layers are only weakly dissipative. In the SI, we also show the results obtained
 208 for the case where the magma ocean is underlain by a 100-km thick, low viscosity “mag-
 209 matic sponge” layer. Comparison of figure 1 with figure S1 in SI indicates that the to-
 210 tal dissipation in the ocean is only weakly sensitive to the viscosity of the sub-oceanic
 211 mantle.

212 The degree of similarity between the predicted heat flux and the observed distri-
 213 bution of Io’s hot spots is illustrated in figures 2b,c. The hot spot distribution is best
 214 fit by a model with $d \approx 5$ km and $\eta = 10^6$ Pa s. This model satisfactorily explains the
 215 hot spots at latitudes below 50° (especially the cluster on the sub-Jovian hemisphere)
 216 but like other magma ocean models, it does not account for hot spots in the polar re-
 217 gions. Highly dissipative models in which tidal heating is concentrated in a narrow equa-
 218 torial zone show no relationship with the current hot spot pattern (figure 2c).

219 The origin and the distribution of tidal heating within Io’s interior remain a sub-
 220 ject of debate. The question could, in principle, be answered by a dedicated mission mak-
 221 ing close flybys of Io and providing new information about Io’s gravity signature. Bierson
 222 and Nimmo (2016) have demonstrated that the tidal Love number k_2 of Io is highly sen-
 223 sitive to the presence of a fluid layer beneath the surface. The value of k_2 should be about
 224 0.5 for Io with a fluid magma ocean and 0.1 if Io’s mantle behaves as a solid (see also
 225 Kervazo et al., 2022). The first value should be regarded as a rough estimate because
 226 it was obtained under the assumption that the dynamic effect of the tidal flow in the ocean
 227 can be neglected.

228 In the absence of a fluid magma ocean, the gravitational response of Io to tidal forc-
 229 ing can be expressed as $V_g(a, \theta, \phi, t) = k_2 V_t(a, \theta, \phi, t - \Delta t_2)$, where a is Io’s radius, V_t
 230 is the tidal potential (equation 4) and Δt_2 is the time lag. The response is described by
 231 only two parameters, k_2 and Δt_2 . If Io has a fluid magma ocean, the tidal deformation
 232 generates a degree-2 flow in the ocean, which is further modulated by the Coriolis effect.
 233 Depending on the parameters of the model, the resulting flow can deform the surface and
 234 internal density interfaces, generating a gravitational signal that is much more complex

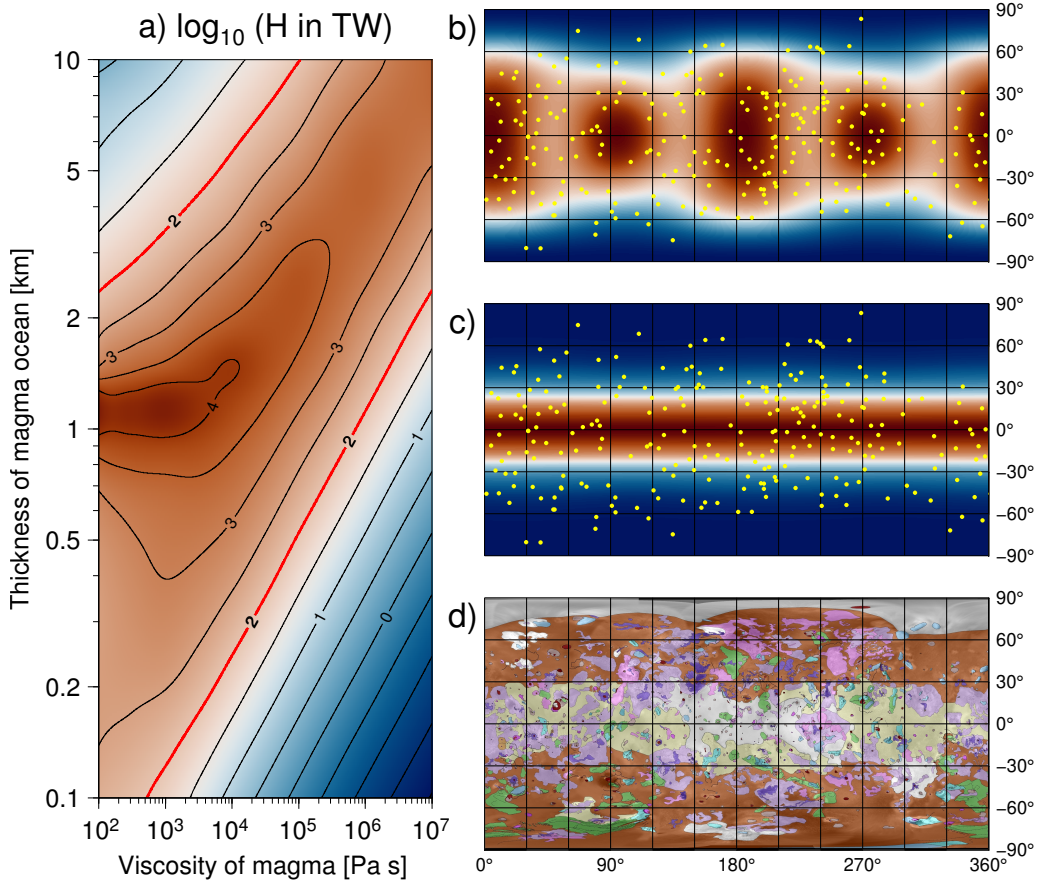


Figure 2. a) Total heat production in the magma ocean as a function of ocean thickness and magma viscosity. The contours plotted in red correspond to Io’s present-day heat production (100 TW). b) Heat flux map that best fits the present-day hot spot distribution (yellow circles, after Davies et al. (2015)). The map is calculated for $\eta = 10^6$ Pa s and $d = 5$ km and corresponds to a total heat production of 3340 TW. About 80% of hotspots are located in a region of higher-than-average heat flux. c) Heat flux map corresponding to the model with the highest dissipation ($2.1 \cdot 10^4$ TW). In this case, only about 50% of hot spots are located in high dissipation regions. d) Geological map of Io (Williams et al., 2011). For the sake of comparison with the geological map, the tidal heat flux in panels b and c is shown in the equidistant cylindrical projection.

235 than in the case of a solid body. The gravitational response at degree 2 varies with the
 236 harmonic order and is described by six parameters, k_{20} , k_{22}^c , k_{22}^s , Δt_{20} , Δt_{22}^c and Δt_{22}^s ,
 237 which can be determined from the following equations (cf. equation 4):

$$238 \quad V_{g,20}(a, t) = k_{20} V_{t,20}(a, t - \Delta t_{20}), \quad (8)$$

$$239 \quad V_{g,22}^c(a, t) = k_{22}^c V_{t,22}^c(a, t - \Delta t_{22}^c), \quad (9)$$

$$240 \quad V_{g,22}^s(a, t) = k_{22}^s V_{t,22}^s(a, t - \Delta t_{22}^s), \quad (10)$$

241 where $V_{g,20}$, $V_{g,22}^c$ and $V_{g,22}^s$ are the coefficients of the gravitational potential induced by
 242 tidal potential coefficients $V_{t,20}$, $V_{t,22}^c$ and $V_{t,22}^s$, respectively.

243 In the case of solid-body tides, $k_{20} = k_{22}^c = k_{22}^s = k_2$ and $\Delta t_{20} = \Delta t_{22}^c = \Delta t_{22}^s =$
 244 Δt_2 . On the other hand, if Io has a magma ocean, the degree-2 Love numbers and time
 245 delays can significantly vary with the order ($m = 0, 2$). While k_{20} increases with the
 246 increasing ocean thickness, reaching a maximum of 0.85 for $d = 10$ km and $\eta = 3 \cdot 10^6$
 247 Pa s (figure 3a), k_{22}^c and k_{22}^s (figure 3b,c) are strongly affected by the Coriolis effect and
 248 correlate with the total heat production (cf. figure 2a). The maximum values of k_{22}^c and
 249 k_{22}^s are about ten times greater than the maximum value of k_{20} . Large differences are
 250 also found between Δt_{20} on one side and Δt_{22}^c and Δt_{22}^s on the other. The values of the
 251 tidal Love numbers and time lags corresponding to Io's current dissipative power (≈ 100
 252 TW) are shown by the red lines. If the ocean thickness is small and/or the magma vis-
 253 cosity is high, $k_{20} \approx k_{22}^c \approx k_{22}^s < 0.1$ and $\Delta t_{20} \approx \Delta t_{22}^c \approx \Delta t_{22}^s < 2$ h, suggesting that,
 254 in this case, the presence of a magma ocean has little effect on the large-scale deforma-
 255 tion of the lithosphere.

256 4 Discussion and conclusions

257 Our results confirm the conclusion of Tyler et al. (2015) that the tidal heating in
 258 a fluid magma ocean can explain Io's observed heat production over a broad range of
 259 magma viscosities and ocean thicknesses. Compared to the studies using the LTE method
 260 (Tyler et al., 2015; Matsuyama et al., 2022), the solution of the Navier-Stokes equations
 261 is characterized by a greater variety of heat flux patterns, which vary depending on the
 262 parameters of the ocean. The highest heat production ($\approx 10^4$ TW, about a hundred times
 263 more than Io's current heat output) is found for models where tidal heating is concen-
 264 trated in an equatorial zone at latitudes below 30° . This heating pattern develops when
 265 the ocean is about 1 km thick and the magma viscosity is about 10^2 Pa s. The distri-

266 bution of the dissipation rate predicted for these parameters is not correlated with the
267 current distribution of hot spots, but it shows a remarkable correspondence with Io's yel-
268 low bright plains, made of silicate and sulphur-rich materials in the form of lava flows
269 buried by pyroclastic deposits (Williams et al., 2011, , see figure 2d). This indicates that
270 Io may have experienced a period of intense tidal heating, accompanied by excessive vol-
271 canism in the equatorial region and leading to catastrophic resurfacing of the pre-existing
272 terrain. The resurfacing event may have been triggered by a temporary increase in Io's
273 eccentricity (Hussmann & Spohn, 2004), resulting in the enhancement of tidal heating
274 and an increase of porosity in a magmatic sponge. The subsequent formation of a magma
275 ocean (Miyazaki & Stevenson, 2022) further increased the tidal dissipation rate in Io's
276 interior and led to a thermal runaway, a positive feedback between temperature and tidal
277 dissipation. Due to the intense tidal heating, the magma production rate was faster than
278 the rate of magma extraction, leading to a rapid increase in the magma ocean thickness
279 and a gradual change in the dissipation pattern and total heat production (see figure 1).
280 The resurfacing event may have been of short duration and was likely to be followed by
281 a rapid decline in resurfacing rate caused by a change in ocean thickness and/or viscos-
282 ity or by a decrease in the eccentricity.

283 The question of whether present-day Io has a magma ocean or not is difficult to
284 answer. It is usually assumed that the Io's volcanic activity should be correlated with
285 the distribution of tidal heating. Magma ocean models (figure 1) predict enhanced tidal
286 heating at low latitudes and low tidal heating in the polar regions. However, new data
287 from the Juno mission indicate that the density of hotspots does not decrease towards
288 the poles (Zambon et al., 2022), in contrast to previous data sets where most of the hot
289 spots were located at low latitudes (e.g., Davies et al., 2015). The low correlation be-
290 tween the hot spots and the predicted tidal heating at high latitudes does not necessar-
291 ily mean that there is no magma ocean on Io. If the ocean is global (i.e., if the magma
292 is stored in a global continuous reservoir), the melt is present everywhere beneath the
293 lithosphere, and the amount of magma that gets to the surface then depends on the lo-
294 cal conditions, rather than on the distribution of tidal heating. In other words, volcanic
295 eruptions can occur at any location where conditions in the lithosphere are favorable for
296 the ascent of magma (Crisp, 1984; Jaeger et al., 2003; de Kleer et al., 2019).

297 Another possible explanation for hot spots in polar regions is the tidal heating in
298 the solid sub-oceanic mantle (Tyler et al., 2015). Unlike dissipation in a liquid ocean,

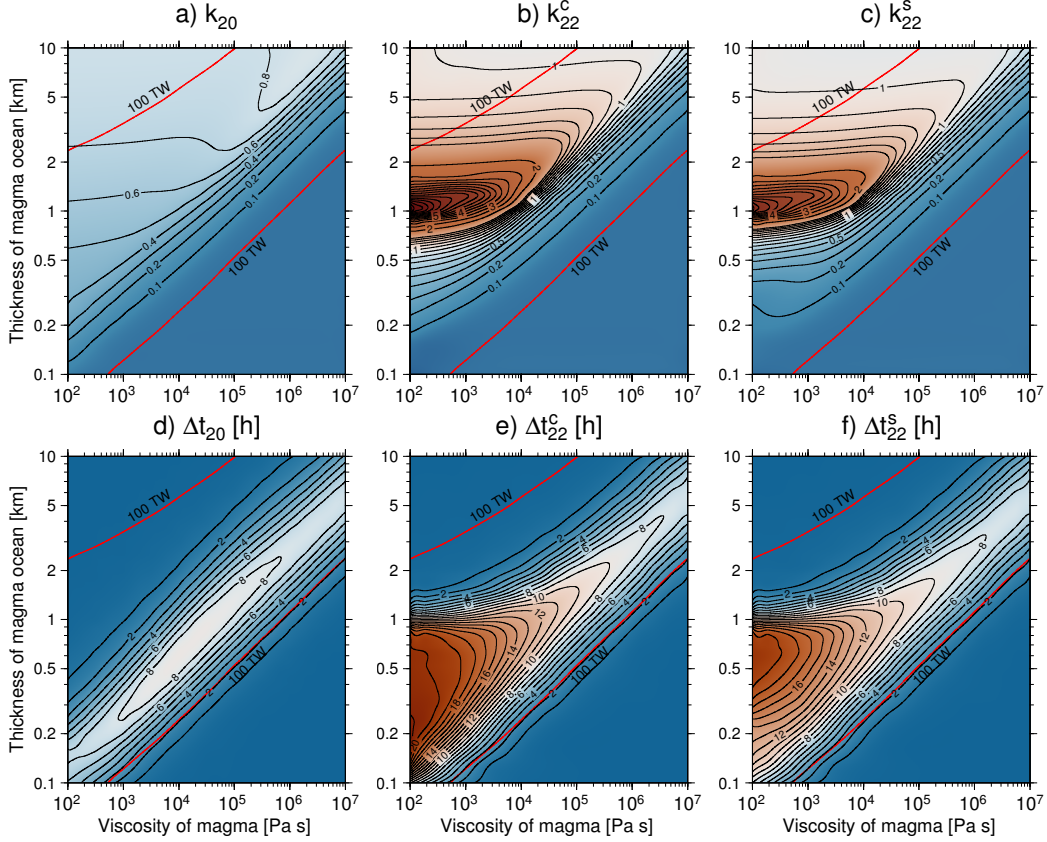


Figure 3. Tidal Love numbers (a–c) and time lags (d–f) as functions of the ocean thickness and magma viscosity. The red lines correspond to models with a heat output of 100 TW. The contour interval in panels a–c is 0.1 if the Love number is less than 1.5 and 0.5 if the Love number is greater than or equal to 1.5. The contour interval in panels d–f is 2 hours.

299 which is concentrated at low latitudes, dissipation in the deep mantle mainly occurs near
 300 the poles (e.g., Tyler et al., 2015; Kervazo et al., 2022; Matsuyama et al., 2022) and, there-
 301 fore, it can compensate for the decrease in ocean tidal heating at high latitudes. If this
 302 is the case, the current distribution of hot spots on Io results from the combined effect
 303 of solid and fluid tidal dissipation (see also figure S2 in SI). However, the question is whether
 304 the heat flux obtained in this way is physically meaningful because the temperature field
 305 in Io’s deep mantle is likely to be affected by convection (Tackley, 2001; Tackley et al.,
 306 2001) and the heat transfer between the solid mantle and the liquid magma ocean can
 307 be modulated by the solid-liquid phase transition (e.g., Labrosse et al., 2018). Finally,
 308 it is possible that the magma ocean has a variable thickness and may even be absent in
 309 some areas. Dissipative behavior of such an ocean is difficult to predict but it is likely
 310 that tidal heating would strongly vary laterally and would be affected by regional res-
 311 onance effects.

312 Bierson and Nimmo (2016) suggested that the presence of a fluid magma ocean on
 313 Io could be detected by measuring the tidal Love numbers. Our results indicate that if
 314 tidal heating preferentially occurs in a magma ocean and the total heat production is
 315 about 100 TW, then the degree-2 Love numbers are either less than 0.1 if $d < 2$ km
 316 (i.e., about the same as in the case of solid tides) or greater than 0.7 if $d > 2$ km. While
 317 in the former case latter case, $k_{22}^c \approx k_{22}^s \approx k_{20}$, in the latter case, k_{22}^c and k_{22}^s are twice
 318 as big as k_{20} . In both cases the time lag is less than 2 hours. The fact that the tidal Love
 319 numbers are not sensitive to the presence of a liquid magma ocean if the ocean thick-
 320 ness is small needs to be taken into account in future analyses of Io’s gravity signature.

321 **Open Research Section**

322 All results presented in the paper can be found in a digital form in Aygün and Čadek
 323 (2023a).

324 **Acknowledgments**

325 B.A. acknowledges the support from the Charles University project SVV 260709.

326 **References**

327 Anderson, J. D., Jacobson, R. A., Lau, E. L., Moore, W. B., & Schubert, G. (2001).
 328 Io’s gravity field and interior structure. *Journal of Geophysical Research-*

- 329 *Planets*, 106, 32963-32969.
- 330 Anderson, J. D., Sjogren, W. L., & Schubert, G. (1996). Galileo gravity results and
331 the internal structure of Io. *Science*, 272, 709-712.
- 332 Aygün, B., & Čadek, O. (2023a). *Data for the article "Tidal heating in a subsurface*
333 *magma ocean on Io revisited"*. Zenodo. Available from [https://doi.org/10](https://doi.org/10.5281/zenodo.10370912)
334 [.5281/zenodo.10370912](https://doi.org/10.5281/zenodo.10370912)
- 335 Aygün, B., & Čadek, O. (2023b). Impact of the core deformation on the tidal heat-
336 ing and flow in Enceladus subsurface ocean. *Journal of Geophysical Research:*
337 *Planets*, 128, e2023JE007907.
- 338 Beuthe, M. (2016). Crustal control of dissipative ocean tides in Enceladus and other
339 icy moons. *Icarus*, 280, 278-299.
- 340 Bierson, C. J., & Nimmo, F. (2016). A test for Io's magma ocean: Modeling tidal
341 dissipation with a partially molten mantle. *Journal of Geophysical Research-*
342 *Planets*, 121, 2211-2224.
- 343 Blöcker, A., Saur, J., Roth, L., & Strobel, D. F. (2018). Mhd modeling of the
344 plasma interaction with Io's asymmetric atmosphere. *Journal of Geophysical*
345 *Research-Space Physics*, 123, 9286-9311.
- 346 Chen, E. M. A., Nimmo, F., & Glatzmaier, G. A. (2014). Tidal heating in icy satel-
347 lites oceans. *Icarus*, 229, 11-30.
- 348 Crisp, J. A. (1984). Rates of magma emplacement and volcanic output. *Journal of*
349 *Volcanology and Geothermal Research*, 20, 177-211.
- 350 Davies, A., Veeder, G., Matson, D., & Johnson, T. (2015). Map of Io's volcanic heat
351 flow. *Icarus*, 262, 67-78.
- 352 de Kleer, K., McEwen, A. S., & Park, R. S. (2019). *Tidal heating: Lessons from Io*
353 *and the Jovian system* (Tech. Rep.). Keck Institute for Space Studies, Caltech,
354 Pasadena.
- 355 Hamilton, C. W., Beggan, C. D., Still, S., Beuthe, M., Lopes, R. M. C., Williams,
356 D. A., et al. (2013). Spatial distribution of volcanoes on Io: Implications for
357 tidal heating and magma ascent. *Earth and Planetary Science Letters*, 361,
358 272-286.
- 359 Hay, H., & Matsuyama, I. (2019). Nonlinear tidal dissipation in the subsurface
360 oceans of Enceladus and other icy satellites. *Icarus*, 319, 68-85.

- 361 Hussmann, H., & Spohn, T. (2004). Thermal-orbital evolution of Io and Europa.
362 *Icarus*, *171*, 391-410.
- 363 Jaeger, W., Turtle, E., Keszthelyi, L., Radebaugh, J., & McEwen, A. (2003). Oro-
364 genic tectonism on Io. *Journal of Geophysical Research-Planets*, *108*, 5093.
- 365 Kaula, W. M. (1964). Tidal dissipation by solid friction and the resulting orbital
366 evolution. *Rev. Geophys.*, *2*, 661-685.
- 367 Kervazo, M., Tobie, G., Choblet, G., Dumoulin, C., & Běhouňková, M. (2021). Solid
368 tides in Io's partially molten interior: Contribution of bulk dissipation. *Astron-
369 omy & Astrophysics*, *650*.
- 370 Kervazo, M., Tobie, G., Choblet, G., Dumoulin, C., & Běhouňková, M. (2022). In-
371 ferring Io's interior from tidal monitoring. *Icarus*, *373*.
- 372 Keszthelyi, L., Jaeger, W., Milazzo, M., Radebaugh, J., Davies, A. G., & Mitchell,
373 K. L. (2007). New estimates for Io eruption temperatures: Implications for the
374 interior. *Icarus*, *192*, 491-502.
- 375 Keszthelyi, L., McEwen, A. S., & Taylor, G. J. (1999). Revisiting the hypothesis of a
376 mushy global magma ocean in Io. *Icarus*, *141*, 415-419.
- 377 Khurana, K. K., Jia, X., Kivelson, M. G., Nimmo, F., Schubert, G., & Russell, C. T.
378 (2011). Evidence of a global magma ocean in Io's interior. *Science*, *332*,
379 1186-1189.
- 380 Labrosse, S., Morison, A., Deguen, R., & Alboussière, T. (2018). Rayleigh-Benard
381 convection in a creeping solid with melting and freezing at either or both its
382 horizontal boundaries. *Journal of Fluid Mechanics*, *846*, 5-36.
- 383 Lainey, V., Arlot, J. E., Karatekin, O., & Van Hoolst, T. (2009). Strong tidal dissi-
384 pation in Io and Jupiter from astrometric observations. *Nature*, *459*, 957-959.
- 385 Matsuyama, I., Beuthe, M., Hay, H., Nimmo, F., & Kamata, S. (2018). Ocean tidal
386 heating in icy satellites with solid shells. *Icarus*, *312*, 208-230.
- 387 Matsuyama, I., Steinke, T., & Nimmo, F. (2022). Tidal heating in Io. *Elements*, *18*,
388 374-378.
- 389 Miyazaki, Y., & Stevenson, D. (2022). A subsurface magma ocean on Io: Exploring
390 the steady-state of partially molten planetary bodies. *Planet. Sci. J.*, *11*, 256.
- 391 Moore, W. B. (2001). The thermal state of Io. *Icarus*, *154*, 548-550.
- 392 Moore, W. B. (2003). Tidal heating and convection in Io. *Journal of Geophysical
393 Research-Planets*, *108*.

- 394 O'Reilly, T. C., & Davies, G. F. (1981). Magma transport of heat on Io: A mecha-
 395 nism allowing a thick lithosphere. *Geophysical Research Letters*, *8*, 313-316.
- 396 Peale, S. J., Cassen, P., & Reynolds, R. T. (1979). Melting of Io by tidal dissipation.
 397 *Science*, *203*, 892-894.
- 398 Philpotts, A. R., & Ague, J. J. (2009). *Principles of Igneous and Metamorphic*
 399 *Petrology* (2nd edition ed.). Cambridge, UK: Cambridge University Press.
- 400 Radebaugh, J., Keszthelyi, L. P., McEwen, A. S., Turtle, E. P., Jaeger, W., & Mi-
 401 lazzo, M. (2001). Paterae on Io: A new type of volcanic caldera? *Journal of*
 402 *Geophysical Research-Planets*, *106*, 33005-33020.
- 403 Requier, J., Trinh, A., Triana, S., & Dehant, V. (2019). Internal energy dissipation
 404 in Enceladus subsurface ocean from tides and libration and the role of inertial
 405 waves. *Journal of Geophysical Research: Planets*, *124*, 2198-2212.
- 406 Renaud, J. P., & Henning, W. G. (2018). Increased tidal dissipation using ad-
 407 vanced rheological models: Implications for Io and tidally active exoplanets.
 408 *Astrophysical Journal*, *857*.
- 409 Ross, M. N., & Schubert, G. (1985). Tidally forced viscous heating in a partially
 410 molten Io. *Icarus*, *64*, 391-400.
- 411 Roth, L., Saur, J., Retherford, K. D., Bloeker, A., Strobel, D. F., & Feldman, P. D.
 412 (2017). Constraints on Io's interior from auroral spot oscillations. *Journal of*
 413 *Geophysical Research-Space Physics*, *122*, 1903-1927.
- 414 Rovira-Navarro, M., Rieutord, M., Gerkema, T., Maas, W., L.R. van der Wal, &
 415 Vermeersen, B. (2019). Do tidally-generated inertial waves heat the subsurface
 416 oceans of Europa and Enceladus? *Icarus*, *321*, 126-140.
- 417 Schenk, P., Hargitai, H., Wilson, R., McEwen, A., & Thomas, P. (2001). The moun-
 418 tains of Io: Global and geological perspectives from Voyager and Galileo. *Jour-*
 419 *nal of Geophysical Research-Planets*, *106*, 33201-33222.
- 420 Segatz, M., Spohn, T., Ross, M. N., & Schubert, G. (1988). Tidal dissipation, sur-
 421 face heat flow, and figure of viscoelastic models of Io. *Icarus*, *75*, 187-206.
- 422 Smith, B. A., Shoemaker, E. M., Kieffer, S. W., & Cook, A. F. (1979). Role of SO₂
 423 in volcanism on Io. *Nature*, *280*(5725), 738-743.
- 424 Souček, O., Hron, J., Běhouňková, M., & Čadek, O. (2016). Effect of the tiger
 425 stripes on the deformation of Saturn's moon Enceladus. *Geophys. Res. Lett.*,
 426 *43*, 7417-7423.

- 427 Spencer, D. C., Katz, R. F., & Hewitt, I. J. (2020). Magmatic intrusions control Io's
428 crustal thickness. *Journal of Geophysical Research-Planets*, *125*.
- 429 Spencer, J. R., Rathbun, J. A., Travis, L. D., Tamppari, L. K., Barnard, L., Martin,
430 T. Z., et al. (2000). Io's thermal emission from the Galileo photopolarimeter-
431 radiometer. *Science*, *288*, 1198-1201.
- 432 Steinke, T., Hu, H., Honing, D., Wal, W. van der, & Vermeersen, B. (2020). Tidally
433 induced lateral variations of Io's interior. *Icarus*, *335*.
- 434 Tackley, P. J. (2001). Convection in Io's asthenosphere: Redistribution of nonuni-
435 form tidal heating by mean flows. *Journal of Geophysical Research-Planets*,
436 *106*, 32971-32981.
- 437 Tackley, P. J., Schubert, G., Glatzmaier, G. A., Schenk, P., Ratcliff, J. T., & Matas,
438 J. P. (2001). Three-dimensional simulations of mantle convection in Io. *Icarus*,
439 *149*, 79-93.
- 440 Tyler, R. H., Henning, W. G., & Hamilton, C. W. (2015). Tidal heating in a magma
441 ocean within Jupiter's moon Io. *Astrophysical Journal Supplement Series*,
442 *218*.
- 443 Veeder, G. J., Davies, A. G., Matson, D. L., Johnson, T. V., Williams, D. A., &
444 Radebaugh, J. (2012). Io: Volcanic thermal sources and global heat flow.
445 *Icarus*, *219*, 701-722.
- 446 Veeder, G. J., Matson, D. L., Johnson, T. V., Blaney, D. L., & Goguen, J. D.
447 (1994). Io's heat flow from infrared radiometry: 1983–1993. *Journal of Geo-*
448 *physical Research: Planets*, *99*, 17095-17162.
- 449 Williams, D. A., Keszthelyi, L. P., Crown, D. A., Yff, J. A., Jaeger, W. L.,
450 Schenk, P. M., et al. (2011). *Geologic map of Io: U.S. Geological Sur-*
451 *vey Scientific Investigations Map 3168, scale 1:15,000,000.* Available at
452 <https://pubs.usgs.gov/sim/3168/>.
- 453 Zambon, F., Mura, A., Lopes, R., Rathbun, J., Tosi, F., Sordini, R., et al. (2022). Io
454 hot spot distribution detected by Juno/JIRAM. *Geophysical Research Letters*,
455 *50*, e2022GL100597.